THE JOURNAL OF BIOLOGICAL CHEMISTRY
Vol. 277, No. 44, Issue of November 1, pp. 41970–41977, 2002

Printed in U.S.A.

Ligand Binding and Structural Analysis of a Human Putative Cellular Retinol-binding Protein*

Received for publication, July 16, 2002, and in revised form, August 8, 2002
Published, JBC Papers in Press, August 9, 2002, DOI 10.1074/jbc.M207124200

Claudia Folli‡, Vito Calderone§¶, Ileana Ramazzina‡, Giuseppe Zanotti§¶‖, and Rodolfo Berni‡ ‡‡**

From the ‡Department of Biochemistry and Molecular Biology, University of Parma, 43100 Parma, Italy, §Department of Organic Chemistry, University of Padova, 35131 Padova, Italy, ¶Biopolymer Research Center, Italian National Research Council, 35131 Padova, Italy, and ‖Venetian Institute of Molecular Medicine, 35129 Padova, Italy

Three cellular retinol-binding protein (CRBP) types (CRBP I, II, and III) with distinct tissue distributions and retinoid binding properties have been structurally characterized thus far. A human binding protein, whose mRNA is expressed primarily in kidney, heart, and transverse colon, is shown here to be a CRBP family member (human CRBP IV), according to amino acid sequence, phylogenetic analysis, gene structure organization, and x-ray structural analysis. Retinol binding to CRBP IV leads to an absorption spectrum distinct from a typical holo-CRBP spectrum and is characterized by an affinity (K_d = ~200 nM) lower than those for CRBP I, II, and III, as established in direct and competitive binding assays. As revealed by mutagenic analysis, the presence in CRBP IV of His^{108} in place of Gln^{108} is not responsible for the unusual holo-CRBP IV spectrum. The 2-Å resolution crystal structure of human apo-CRBP IV is very similar to those of other structurally characterized CRBPs. The side chain of Tyr^{60} is present within the binding cavity of the apoprotein and might affect the interaction with the retinol molecule. These results indicate that human CRBP IV belongs to a clearly distinct CRBP subfamily and suggest a relatively different mode of retinol binding for this binding protein.

Vitamin A is an essential micronutrient that plays a key role in vision, cell growth and differentiation, and embryonic development. Because of its chemical instability and quite low solubility in the aqueous medium, the retinol molecule needs to be bound by specific binding proteins in body fluids and within the cell. Cytoplasmic carriers of the retinol molecule are monomeric proteins of ~15.5 kDa, the cellular retinol-binding proteins (CRBPs)[1] (for reviews, see Refs. 1 and 2). They belong to a superfamily of small cytoplasmic proteins that interact specifically with hydrophobic ligands, the intracellular lipid-binding proteins (iLBPs). Besides CRBPs, well-characterized members of the iLBP superfamily are the cellular retinoic acid-binding proteins (CRABPs) and the fatty acid-binding proteins (FABPs). Despite the fact that members of the different protein families may possess a low sequence identity, a basic structural motif has been found for the iLBPs characterized thus far (for reviews, see Refs. 3 and 4). In all these proteins, 10 β-strands (A–J) and two α-helices (I and II) fold to form a well-defined β-barrel, the internal cavity of which contains the binding site for the hydrophobic ligand. The properties of rat CRBP I and II have been investigated extensively (1, 2, 5–9). A number of studies have provided evidence for an important role of CRBPs in vitamin A homeostasis. Specifically, *in vitro* studies have suggested that CRBP I is involved in retinol internalization and intercellular transfer (10–12), retinol esterification (13–15), retinyl ester hydrolysis (10, 16), and the oxidation of retinol to retinaldehyde, a key step of retinoic acid biosynthesis (17, 18). A recent *in vivo* study has shown that retinol esterification and intercellular retinol transfer between liver cells are strongly impaired in CRBP I-null mice, suggesting a key role of CRBP I in these two processes (19). CRBP II, a protein essentially confined to the small intestine, supports efficient retinol esterification (15). It has been proposed that CRBP II is involved specifically in the intestinal absorption and/or metabolism of retinoids.

Recently, a putative CRBP, human CRBP III, has been identified, heterologously expressed, and structurally characterized (20). This protein has been shown to interact specifically with retinol *in vitro*, producing a characteristic absorption spectrum quite similar to those of rat holo-CRBP I and II. A murine iLBP, the amino acid sequence of which suggests that it belongs to the CRBP family, has also been recently identified and heterologously expressed (21, 22). This protein, which was designated murine CRBP III (22) but is well distinct from human CRBP III (20), was reported to interact with retinol, as shown by the enhancement of retinol fluorescence associated with the binding of the vitamin to the apoprotein (22). We report here the identification, ligand binding, tissue distribution, and crystal structure of a human putative CRBP, which is very closely related phylogenetically to murine CRBP III.

* This study was supported by research grants from the Consiglio Nazionale delle Ricerche, Rome, Italy (to G. Z.), Target Project on Biotechnology of the Consiglio Nazionale delle Ricerche, Rome, Italy, and Cofin 2000 (to R. B.) and Cofin 2001 (to R. B. and G. Z.) of the Ministero dell'Istruzione, Universita' e Ricerca, Rome, Italy. The costs of publication of this article were defrayed in part by the payment of page charges. This article must therefore be hereby marked "*advertisement*" in accordance with 18 U.S.C. Section 1734 solely to indicate this fact.

The atomic coordinates and structure factors (code 1LPJ) have been deposited in the Protein Data Bank, Research Collaboratory for Structural Bioinformatics, Rutgers University, New Brunswick, NJ (http://www.rcsb.org/).

The nucleotide sequence(s) reported in this paper has been submitted to the GenBank™ with accession number(s) AY145438.

** To whom correspondence may be addressed: Dept. of Organic Chemistry, University of Padova, Via Marzolo 1, 35131 Padova, Italy. Tel.: 39-049-8275245; Fax: 39-049-8275239; E-mail: giuseppe.zanotti@unipd.it.

‡‡ To whom correspondence may be addressed: Dept. of Biochemistry and Molecular Biology, University of Parma, Parco Area delle Scienze, 23/A, 43100 Parma, Italy. Tel.: 39-0521-905645; Fax: 39-0521-905151; E-mail: rodolfo.berni@unipr.it.

[1] The abbreviations used are: CRBP, cellular retinol-binding protein; iLBP, intracellular lipid-binding protein; CRABP, cellular retinoic acid-binding protein; FABP, fatty acid-binding protein; r.m.s.d., root mean square deviation.

EXPERIMENTAL PROCEDURES

Materials—Recombinant human CRBP III was prepared as described previously (20). Recombinant rat CRBP II was a kind gift of D. Cavazzini. All-*trans*- and 13-*cis*-retinol, all-*trans*- and 13-*cis*-retinaldehyde, and all-*trans*-retinoic acid were purchased from Sigma. Crystal Screen 1 and 2 were obtained from Hampton Research. All other chemicals were of analytical grade.

Identification, Bacterial Expression, and Purification of Human CRBP IV—The expressed sequence tag data base was screened with the BLAST program (23) by using the complete coding sequences of human CRBP I, CRBP II, and CRBP III as queries. A human complete cDNA from lung carcinoid highly similar to CRBPs was identified in the expressed sequence tag sequence AI694572. The clone containing the expressed sequence tag sequence AI694572 in plasmid pT7T3D-Pac was purchased from American Type Culture Collection and sequenced on both strands by the dideoxy chain termination method (24). The region of plasmid pT7T3D-Pac corresponding to the entire human CRBP coding sequence (402 bp) was PCR-amplified using a high-fidelity thermostable DNA polymerase (*Deep Vent* DNA polymerase; Biolabs) and two sequence-specific primers, an *Nde*I-tailed upstream primer (5′-CTCATATGCCCGCCGACCTCAGC-3′) and a *Bam*HI-tailed downstream primer (5′-TTGGATCCTCAGGCTCTCTGGAATGTCTG-3′). After the addition of 3′-terminal adenosine residues by incubation for 30 min at 72 °C in the presence of *Taq* DNA polymerase (PerkinElmer Life Sciences), the amplification product was inserted into the pGEM vector (Promega) to generate the intermediate vector pGEM-CRBP IV. The restriction fragment obtained from *Nde*I/*Bam*HI digestion of plasmid pGEM-CRBP IV was then ligated into the dephosphorylated *Nde*I and *Bam*HI sites of the expression vector pET11b (Novagen), and the resulting plasmid (pET-CRBP IV) was electroporated into *Escherichia coli* BL21 (DE3) cells. The expression of human CRBP IV was induced by adding 1 mM isopropyl-1-thio-β-D-galactopyranoside; after incubation for 2 h and 30 min at 25 °C, cells were lysed by ten 15-s bursts of sonication. CRBP IV was purified to homogeneity, as assessed on a 15% SDS-PAGE gel, using a two-step procedure consisting of gel filtration and anion exchange chromatography (25), with a final yield of ~1.5 mg/liter cell culture. The $\epsilon_{280\ nm}$ (extinction coefficient) of human CRBP IV, calculated on the basis of its predicted amino acid sequence (26), was estimated to be 25,800 $M^{-1}cm^{-1}$.

Sequence Analyses—Multiple amino acid sequence alignments were constructed using the CLUSTALW program (27). Phylogenetic analyses were performed with the CLUSTALX program (version 1.8; NCBI). Genetic distances were analyzed with the neighbor-joining algorithm. The exon-intron structures of human iLBP genes were analyzed by comparing genomic sequences with cDNA sequences by means of the BLAST program (23).

Expression and Purification of Recombinant Human CRBP I—The region of the plasmid pUC18 corresponding to the entire human CRBP I coding sequence (405 bp) was PCR-amplified using a high-fidelity thermostable DNA polymerase (*Deep Vent* DNA polymerase; Biolabs) and two sequence-specific primers, a *Nco*I-tailed upstream primer (5′-CCATGGCAGTCGACTTCACTGGG-3′) and an *Eco*RI-tailed downstream primer (5′-GCTGTGCAAAGAGGAATTCTGGC). After preparation of the intermediate vector pGEM-CRBP I, the restriction fragment obtained from *Nco*I/*Eco*RI digestion was ligated into the dephosphorylated *Nco*I/*Eco*RI sites of expression vector pET28b (Novagen). The correct cDNA sequence encoding human CRBP I was obtained by site-directed mutagenesis using the following primers: CRBP I upstream primer, 5′-GGAGATATACCATGCCAGTCGACTTCAGTGGG-3′; and CRBP I downstream primer, 5′-CCCAGTGAAGTCGACTGGCATGGTATATCACC-3′. Because the mutagenic oligonucleotides delete the *Nco*I restriction site, the occurrence of the desired mutation could be verified by restriction analysis by means of *Nco*I digestion. Single clones were then sequenced to confirm the correctness of the sequence. Finally, the plasmid was electroporated into *E. coli* BL21 (DE3) cells, and the protein was expressed and purified as described above for CRBP IV, with a final yield of ~3 mg/liter cell culture.

Site-directed Mutagenesis—The CRBP IV/H108Q and CRBP I/Q108H mutations were obtained by using a high-fidelity thermostable DNA polymerase (*PfuTurbo* DNA polymerase; Stratagene). The plasmids pET11b-CRBP IV and pET28b-CRBP I were used as template, and two mutagenic primers complementary to opposite strands were synthesized: CRBP IV upstream primer (5′-GAACAGAGGCTGGACCCAGTGGATCGAAGG-3′) and CRBP IV downstream primer (5′-CCCTTCGATCCACTGGGTCCAGCCTCTGTTC-3′), and CRBP I upstream primer (5′-GCTGGACCCACTGGATCGAGGGTGATGAGC-3′) and CRBP I downstream primer (5′-GCTCATCACCCTCGATCCAGTGGGTCCAGC-3′). The products of reaction were treated with *Dpn*I (Stratagene) to digest the parental DNA template. This procedure allowed selection of the clones carrying newly synthesized and potentially mutated plasmids. The products of each digestion were used to transform *E. coli* XL1 Blue cells. Single clones were then sequenced to confirm the occurrence of the desired mutation. Finally, mutant plasmids were electroporated into *E. coli* BL21 (DE3) cells, and mutant proteins were expressed and purified as described for the native proteins.

TABLE I
Data collection and refinement statistics[a]

Space group	C2 (1 molecule/asymmetric unit)
Cell dimensions	a = 34.052 Å b = 57.186 Å c = 67.940 Å β = 104.032°
Resolution (Å)	28.6−2.0 (2.11−2.0)
Total reflections	19128
Unique reflections	7611
Overall completeness (%)	89.6 (91.4)
R_{sym} (%)	12.4 (38.2)
Multiplicity	2.7 (2.7)
$<I/\sigma(I)>$	3.8 (1.3)
Total reflections used	7576 (1126)
Reflections in working set	6767 (990)
Reflections in test set	809 (136)
R_{cryst}	23.4 (25.4)
R_{free} (%)	27.6 (30.0)
Protein atoms	1084
Water molecules	150
r.m.s.d. on bond lengths, Å	0.007
r.m.s.d. on bond angles, °	1.400

[a] Numbers in parentheses refer to the last resolution shell.

Ligand Binding Assays—Recombinant binding proteins (≈5 × 10^{-6} M) in 50 mM potassium phosphate (pH 7.3) and 150 mM NaCl were supplemented with 1.5 equivalents of all-*trans*-retinol or other retinoids dissolved in ethanol and stirred gently in the spectrophotometer cuvette. After a few minutes in the dark at room temperature, absorption spectra were recorded with a Varian Cary 1E spectrophotometer. The interaction of retinol with CRBP IV was also investigated by fluorescence titrations carried out with a PerkinElmer Life Sciences LS-50B spectrofluorometer. Retinol binding to apo-CRBP IV was monitored by measuring the quenching of protein fluorescence (excitation, 280 nm; emission, 330 nm). Aliquots (0.2–1 μl) of an ethanolic stock solution of all-*trans*-retinol ($\epsilon_{325\ nm}$ = 46,000 M^{-1} cm^{-1}) were added to a cuvette containing CRBP IV in 50 mM potassium phosphate (pH 7.3) and 150 mM NaCl. After each addition, the protein solution was stirred gently and allowed to equilibrate at 20 °C in the dark for a few minutes before spectrofluorometric analysis. Binding data were analyzed as described previously (25) using Sigma Plot (Jandel, Corte Madera, CA). In competition binding experiments, absorption spectra of human CRBP IV (4 × 10^{-6} M), saturated with 0.7 equivalent of all-*trans*-retinol in 50 mM potassium phosphate (pH 7.3) and 150 mM NaCl, were recorded before and after the addition of equimolar quantities of either human apo-CRBPI, rat apo-CRBP II, or human apo-CRBP III.

Crystallization, Data Collection, and Structure Determination—Single crystals of apo-CRBP IV were obtained at 18 °C in 2–3 weeks, using the sitting drop vapor-diffusion method, from a solution containing 10% (w/v) PEG 4000, 10% (v/v) 2-propanol, and 50 mM sodium citrate (pH 5.6). After equilibration, the protein concentration was ~8 mg/ml. A single crystal (~0.02 × 0.02 × 0.02 mm) was frozen under nitrogen at 100 K in the presence of the crystallization mother liquid supplemented with 10% (v/v) glycerol as cryoprotectant. Diffraction data were collected at the synchrotron beam line ID29 of European Synchrotron Radiation Facility (Grenoble, France), using a Quantum 4R detector and a wavelength of 0.9184 Å. The crystal to detector distance was 190 mm, and the oscillation was 1°. A native data set could be collected at a maximum resolution of 2.0 Å. Data indexing and integration were performed with the Mosflm program (28), and scaling and merging were performed with the Scala program (28). The crystal structure was solved by the molecular replacement method with AmoRe software (29), by using the structure of rat holo-CRBP I as a template (5). The residues of human CRBP IV that are different relative to rat CRBP I were then replaced according to the CRBP IV sequence. The structure was refined with the programs CNS (30) and SHELX (31). Visualization of the model and manual rebuilding were performed with XtalView (32). The quality of the final models was assessed using the PROCHECK program (33). Solvent molecules were added in the final stages of refinement according to hydrogen bond criteria. The interior of the

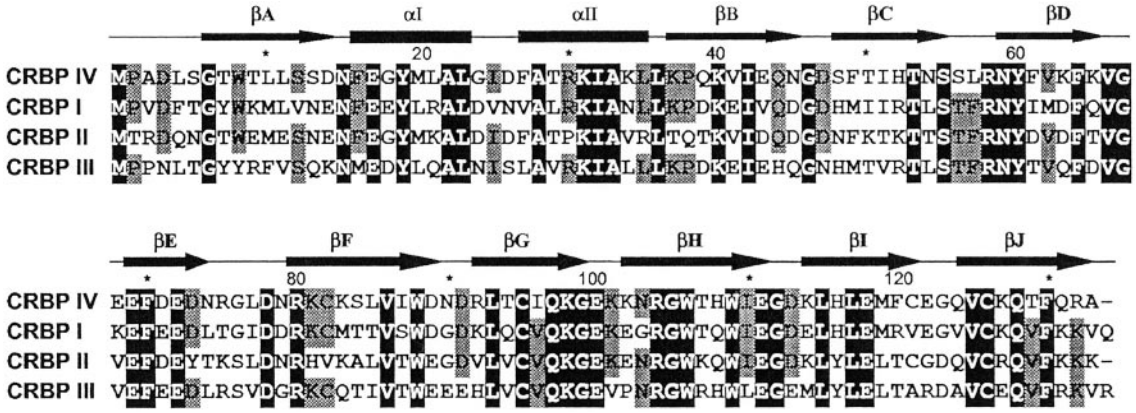

FIG. 1. **Multiple amino acid sequence alignment between human CRBP IV and previously characterized human CRBPs.** Residues that are identical in four or three of the four sequences are *boxed* in *black* or *gray*, respectively. The positions of β-strands A–J (*arrows*) and α-helices I and II (*boxes*) are indicated according to Cowan *et al.* (5). Accession numbers for human CRBPs are reported in Table II.

protein cavity showed some elongated density (see "Discussion"), and solvent molecules were fitted in it. Stereochemical parameters are as expected for molecular models at this resolution: 81.7% of residues are in the most-favored regions of the Ramachandran plot, with 15.0% in additionally allowed regions and 3.3% in generously allowed regions. The overall G factor is 0.0. Data collection and refinement statistics are shown in Table I.

RNA Blot Analysis—A cDNA fragment corresponding to the 3′-untranslated region of human CRBP IV mRNA was generated by PCR and used as a transcript-specific CRBP probe. The CRBP IV (187 bp) probe was amplified under standard PCR conditions by using a plasmid containing the corresponding full-length cDNA as template. The sequences of the oligonucleotide primers used for amplification were as follows: upstream primer, 5′-TCCACATCCAGCAGCAGAGCC-3′, and downstream primer, 5′-GGACAGGTTTATTGAAGCTGAGC-3′. Radioactively labeled probe with a specific activity of about 150 μCi/pmol (1 Ci = 37 GBq) was prepared with the Prime-a-Gene® Labeling System (Promega) by using [α-^{32}P]dCTP as the labeling precursor. A multiple tissue RNA dot-blot (Clontech) containing polyadenylated RNAs from 64 different human tissues and 8 tumor cell lines arrayed on a nylon membrane was used to analyze the expression pattern of human CRBP IV mRNA. Prehybridization and hybridization were carried out according to the manufacturer's instructions. Approximately 24 × 10^6 cpm equivalents of the probe were used for hybridization. The first four washes were done at 65 °C for 20 min with 2× SSC buffer (0.15 M sodium chloride, 0.015 M sodium citrate, pH 7) containing 1% SDS, and the final four washes were done at 55 °C for 20 min with a 0.1× SSC buffer containing 0.5% SDS. Hybridization signals were quantified from phosphorimages recorded with a Personal Molecular Imager FX (Bio-Rad) by using the program QUANTITY-ONE.

RESULTS

Identification, Phylogenetic Analysis, and Gene Structure of Human CRBP IV—A similarity search against the entire expressed sequence tag data base, using the amino acid sequences of human CRBPs as queries, led to the identification of a full-length cDNA from human lung carcinoid. Based on the amino acid sequence deduced from such cDNA (shown in Fig. 1), the estimated molecular mass of the encoded protein (15.5 kDa) was typical of an iLBP. This amino acid sequence is significantly more similar to those of previously identified CRBPs than to those of the other members of the iLBP superfamily (Table II), strongly suggesting that the novel protein belongs to the CRBP family. Specifically, this protein, designated human CRBP IV, shares a higher sequence identity with human CRBP I (57%) and II (58%) than with human CRBP III (49%). A quite high sequence identity (89%) is shared with murine CRBP III (21, 22), clearly indicating that human CRBP IV is most likely the human ortholog of murine CRBP III. It is worth noting that the sequence identities shared by CRBP IV and the other human CRBP types are comparable to those shared by human CRBP I and II (54%), human CRBP I and III (56%), and human CRBP II and III (50%) pairs. A phylogenetic tree for CRBPs, including zebrafish (34) and gecko (*Lygodactilus picturatus*) (35) CRBPs, has been constructed, indicating that human CRBP IV is related more closely to human CRBP II than to human CRBP I and III (Fig. 2). Interestingly, in this phylogenetic tree, zebrafish CRBP clusters with human CRBP II (74% sequence identity), whereas gecko CRBP clusters with human CRBP III (62% sequence identity). Gene organization for iLBPs is very similar, with the transcription unit split into four exons and three introns. Remarkably, the size of translated exon sequences and intron position are highly conserved in the genes of human CRBPs, including the gene of the newly identified human CRBP IV (Fig. 3).

TABLE II
Comparison between human CRBP IV and other members of the iLBP superfamily in order of descending amino acid sequence identity

iLBP member	Identity (%)	GenBank™ or SwissProt accession no.
Murine CRBP III	89	NP_071303
Human CRBP II	58	P50120
Human CRBP I	57	P09455
Human CRBP III	49	P82980
Human HFABP	40	1714345A
Human mP2	38	P02689
Human CRABP II	38	P29373
Human CRABP I	36	P29762

Retinol Binding to Recombinant Wild-type and Mutant Forms of Human CRBP IV—A protein with a molecular mass close to that expected for CRBP IV has been overexpressed in *E. coli* cells transformed with a pET-CRBP IV plasmid (see "Experimental Procedures" for details). This protein has been purified to homogeneity and utilized for retinol binding experiments. The addition of all-*trans*-retinol to human apo-CRBP IV produces an absorption spectrum clearly distinct from those of both free retinol and retinol bound to previously characterized CRBP types and with an absorbance intensity in the 300–400 nm region lower than that of the protein at 280 nm. The spectra of human holo-CRBP I and IV, obtained in the presence of a slight molar excess of all-*trans*-retinol, are compared in Fig. 4*A*. The spectrum of holo-CRBP IV displays fine structure, as in the case of holo-CRBP I, but exhibits relatively smooth and shifted peak and shoulders. The presence of fine structure in the 300–400 nm region is consistent with the retinol β-ionone ring being planar with the polyene chain, as suggested for rat holo-CRBP I in solution (36) and confirmed for the same holoprotein in the crystal state (5). The lower absorbance intensity in the 300–400 nm region of holo-CRBP IV as compared with other holo-CRBPs indicates an undersatu-

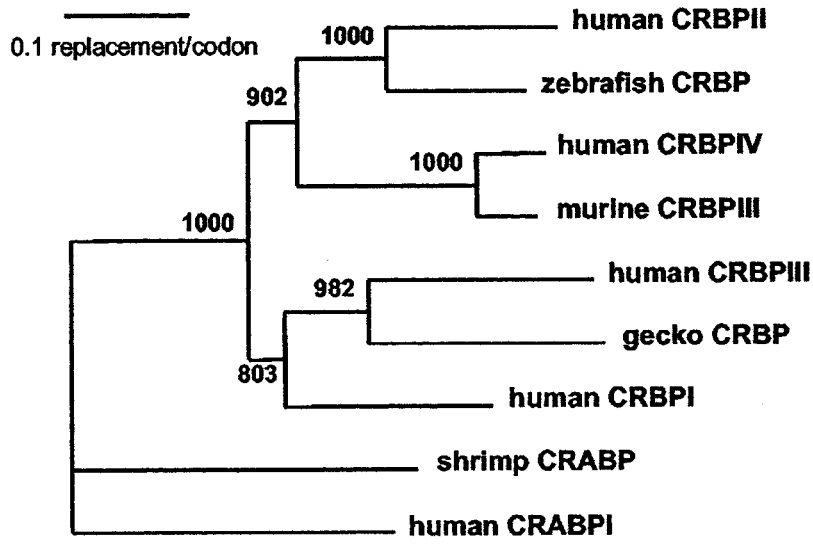

FIG. 2. **Phylogenetic tree for CRBPs.** The neighbor-joining method has been used for phylogenetic tree construction. The sequence of human CRABP I was used as outgroup. Bootstrap scores are based on 1000 replicates. GenBank™ or SwissProt accession numbers are as follows: P29762, human CRABP I; AF458289, shrimp (*Metapenaeus ensis*) CRABP; AF448140, zebrafish (*Danio rerio*) CRBP; AJ249753, diurnal gecko (*L. picturatus*) CRBP; and NP_071303, murine CRBP III. Accession numbers for human CRBPs are reported in Table II.

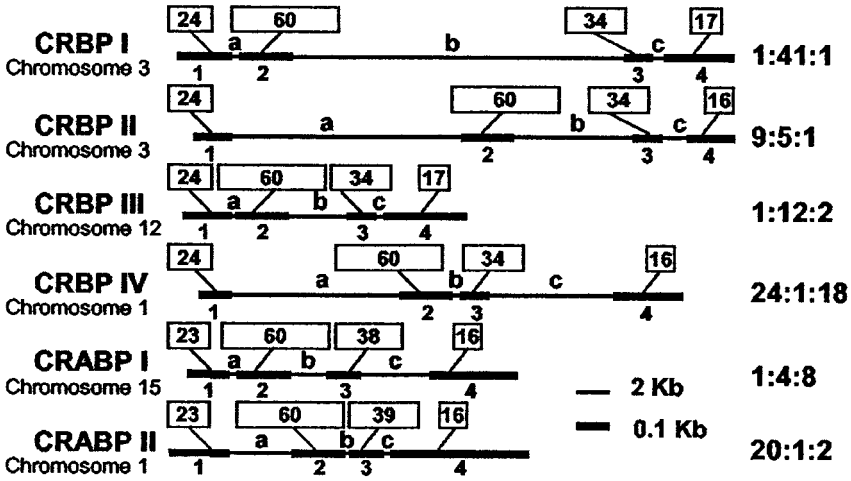

FIG. 3. **Schematic diagram representing gene structure organization for human CRBPs.** Genes are aligned at their methionine initiator codon (ATG). Exons (*1–4*) and introns (*a–c*) are shown as *bold lines* and *thin lines,* respectively. Translated exon sequences are enlarged, and their size, expressed as the number of encoded amino acid residues, is denoted by *boxed numbers*. Relative intron size (ratio, *a:b:c*) is listed to the *right* of each gene. For a comparison, gene organization for human CRABP I and II is shown also.

rated binding stoichiometry of CRBP IV. An undersaturation of CRBP IV by retinol might be caused by the presence inside the retinol binding cavity of nonspecifically bound ligand/ligands competing with the retinol molecule, as suggested by the x-ray analysis of apo-CRBP IV (see below). However, attempts to extract nonspecifically bound ligands from apo-CRBP IV by means of a hydrophobic resin (Lipidex) or organic solvents did not lead to a larger 300–400 nm absorbance of holo-CRBP IV (data not shown). The atypical absorption spectrum of holo-CRBP IV is consistent with a rather distinct mode of binding of retinol. This spectrum cannot be compared with that of retinol complexed with the orthologous murine CRBP III. In fact, no absorption spectrum was presented for all-*trans*-retinol bound to murine CRBP III, whereas an increase in retinol fluorescence was shown to occur as a result of the interaction of the vitamin with the murine protein (22).

Spectrofluorometric titrations of CRBPs by retinol can be carried out by exploiting the decrease in intrinsic protein fluorescence that is brought about by energy transfer from excited tryptophans to protein-bound retinol. A typical fluorescence titration curve of human CRBP IV with all-*trans*-retinol, shown in Fig. 4*C,* reveals a moderately low binding affinity for retinol. In fact, a binding curve corresponding to an apparent dissociation constant of about 200 nM and a binding stoichiometry of about 0.5 retinol-occupied site/CRBP IV molecule were found to fit the experimental data best. Competition binding experiments have also been carried out to compare the affinity of human CRBP IV with those of CRBP I, II, and III for all-*trans*-retinol (Fig. 5). The basis for these experiments is that the absorption spectrum of all-*trans*-retinol bound to CRBP IV is distinguishable from the absorption spectra of all-*trans*-retinol bound to the other CRBP types. The spectrum of human apo-CRBP IV preincubated with 0.7 equivalent of all-*trans* retinol was recorded; the subsequent addition of equimolar quantities of either human apo-CRBP I (Fig. 5*A*), rat apo-CRBP II (Fig. 5*B*), or human apo-CRBP III (Fig. 5*C*) led to the appearance of absorption spectra typical of the complexes of retinol with CRBP I, II, and III, respectively. These results are consistent with an affinity of retinol for CRBP IV that is substantially lower than that for the other CRBP types.

Several amino acid residues in close contact with retinol in holo-CRBPs or presumed to be in close contact with retinol in as-yet-uncharacterized holoproteins are identical or chemically conserved within the CRBP family, with the exception of Gln^{108}, which is replaced by a His residue in human CRBP III (20). Similar to human CRBP III, human CRBP IV has a His residue at position 108. To evaluate the role of the Gln/His residue at position 108 in the interaction with retinol, the CRBP I/Q108H and CRBP IV/H108Q mutants have been obtained. Based on the nearly identical absorption spectra of the wild-type and mutant forms of holo-CRBP IV, as well as the wild-type and mutant forms of holo-CRBP I (Fig. 4, *A* and *B*), the interactions of all-*trans*-retinol with mutant forms are likely to be highly similar to those present in the corresponding wild-type holoproteins. Therefore, a His residue at position 108 in CRBP I is likely to hydrogen bond the retinol hydroxyl end

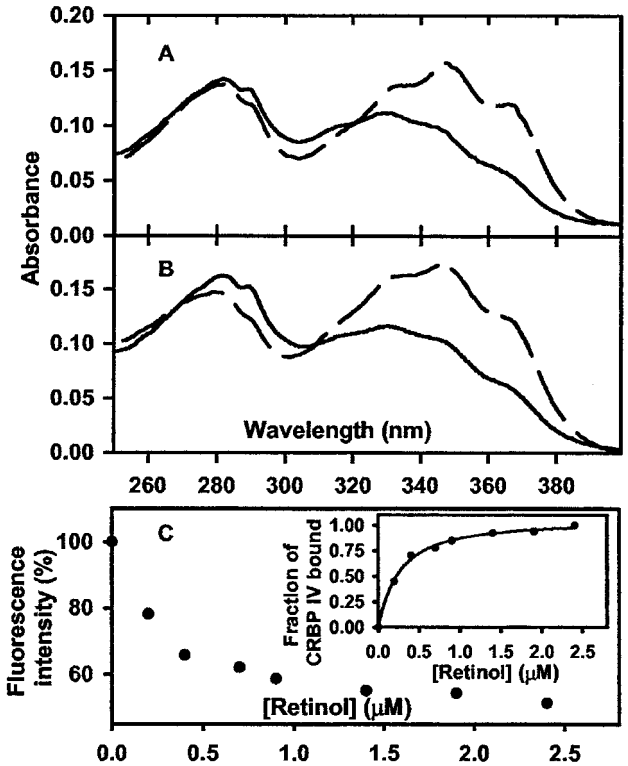

FIG. 4. **Retinol binding to human apo-CRBP IV.** *A*, absorption spectra of the complexes of retinol with wild-type human CRBP IV (*solid line*) and human CRBP I (*dashed line*). *B*, absorption spectra of the complexes of retinol with human CRBP IV/H108Q mutant (*solid line*) and human CRBP I/Q108H mutant (*dashed line*). Absorption spectra were recorded after the addition of a slight molar excess of all-*trans*-retinol to the recombinant apoproteins (5×10^{-6} M), followed by equilibration in the dark for a few minutes at 20 °C. *C*, spectrofluorometric titration of human apo-CRBP IV with retinol at 20 °C. Intrinsic protein fluorescence (percentage) of apo-CRBP IV (0.5 μM) is plotted as a function of retinol concentration. *Inset*, fitting of the experimentally determined fractional saturation to a theoretical curve corresponding to the binding of 0.53 mol ligand/mol CRBP IV, with an apparent dissociation constant of 200 nM.

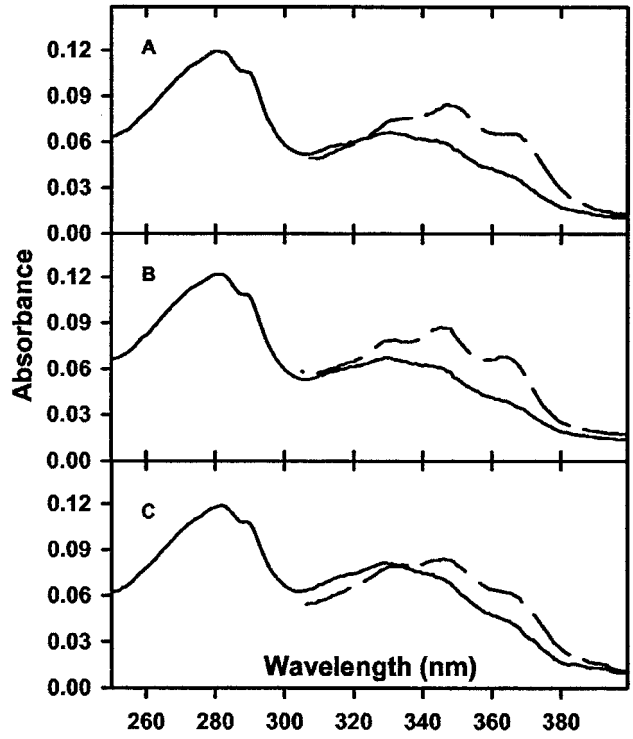

FIG. 5. **Competition between human CRBP IV and previously characterized CRBPs for all-*trans*-retinol.** Absorption spectra of human CRBP IV (4×10^{-6} M) saturated with 0.7 equivalent of *all-trans*-retinol were recorded before (*A*–*C*, *solid line*) and after the addition of equimolar quantities of either human apo-CRBP I (*A*, *dashed line*), rat apo-CRBP II (*B*, *dashed line*), or human apo-CRBP III (*C*, *dashed line*).

group, as established for Gln^{108} of CRBP I and II (5, 6), producing an effective retinol-CRBP interaction. Because the spectrum typical of retinol bound to CRBPs is not restored by the H108Q mutation in CRBP IV, it is concluded that as-yet-unidentified factors, other than the presence of a His residue at position 108, are responsible for the unusual spectrum of holo-CRBP IV.

Three-dimensional Structure of Human Apo-CRBP IV—The x-ray molecular structure of human apo-CRBP IV at 2.0 Å resolution closely resembles the x-ray models of previously characterized CRBPs (Fig. 6, *A* and *B*). The superposition of the α-carbon atoms with the corresponding α-carbon atoms of other iLBPs suggests that human CRBP IV is a CRBP family member. The overall r.m.s.d. between equivalent α-carbon of CRBP I, II, III, and IV is in fact rather small and increases significantly when CRBP IV is compared with other members of the iLBP superfamily (Table III). The relative position of the residues lining the binding cavity in CRBP IV is quite well conserved. The superposition of the side chains of some of the residues that line the retinol-binding site in CRBP II (6) with the corresponding residues in CRBP IV is shown in Fig. 6*C*. The position in the CRBP IV structure of the His^{108} residue replacing the Gln residue that in holo-CRBP I and II hydrogen bonds the retinol hydroxyl end group is remarkable (5, 6). In fact, its imidazole ring is at hydrogen bond distance from the hydroxyl group of a hypothetical retinol molecule bound to CRBP IV with the same conformation as in holo-CRBP I and II. The only significant difference is found for the side chain of Tyr^{60}, the orientation of which is such that it occupies some of the space where the retinol β-ionone ring is positioned within the binding cavity of holo-CRBP I and II (Fig. 6*C*).

Tissue Distribution of Human CRBP IV mRNA—The tissue distribution of human CRBP IV mRNA was analyzed by using a gene-specific DNA probe and an internally normalized dot-blot containing polyadenylated RNAs from 64 different human tissues and 8 tumor cell lines (Fig. 7). Based on the intensities of hybridization signals produced by the CRBP IV probe, we determined the expression pattern of the CRBP IV mRNA. As shown in Fig. 7, the CRBP IV messenger was detected in nearly all human tissues, with the highest abundance in adult kidney, heart, and transverse colon, as well as fetal heart and spleen. High levels of expression were also detected in adult lymph node, appendix, and ascending colon. With regard to the adult heart, the interventricular septum and the apex of the heart were the richest tissues. The signal measured for the adult heart was about 50% of that measured for the adult kidney, at variance with the abundance of the CRBP IV mRNA for fetal kidney, which was about 30% of that found for fetal heart.

DISCUSSION

CRBPs are cytoplasmic retinol-binding proteins that are thought to play an important role in retinol uptake, storage, and metabolism. Mammalian CRBP I and II are the best-characterized members of the CRBP family. The absorption spectra of rat CRBP I and II complexed with their endogenous ligand, all-*trans*-retinol, have been found to be quite similar and are characterized by a peculiar fine structure (36, 37). Recently, two putative CRBPs, which were both designated CRBP III but are two distinct CRBP types, have been identified and heterologously expressed: human CRBP III (20) and murine CRBP III (21, 22). Although retinol has been proposed to

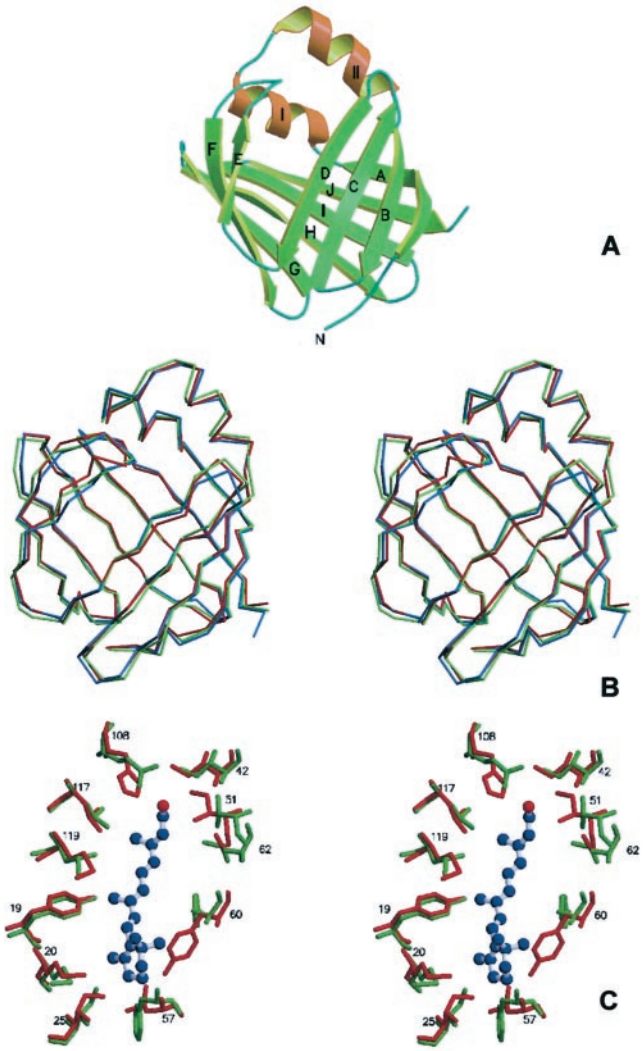

FIG. 6. **Structure of apo-CRBP IV.** *A,* ribbon diagram representing the crystal structure of human apo-CRBP IV. Barrel forming β-strands are in *green*, and the two α-helices are in *orange*. *B,* stereo representation showing the superposition of the Cα chain traces of human CRBP IV (*red*; this work) with rat holo-CRBP I (*blue*; Protein Data Bank identification code 1CRB) and rat-holo-CRBP II (*green*; Protein Data Bank identification code 1OBP). *C,* stereo representation showing the superposition of several residues lining the retinol-binding site in rat apo-CRBP II (*green*; Protein Data Bank identification code 1OPA) with the corresponding residues in human apo-CRBP IV (*red*). The retinol molecule (*ball-stick model*), as it is bound in rat holo-CRBP II, is shown also.

TABLE III
Overall r.m.s.d. between α-carbon atoms of CRBP IV and corresponding atoms of other iLBPs

CRBP IV *vs.*	r.m.s.d. (Å)[a]	Protein Data Bank identification code
Rat holo-CRBP I	0.8	1CRB
Rat apo-CRBP II	0.8	1OPA
Rat holo-CRBP II	0.7	1OPB
Human apo-CRBP III	0.9	1GGL
Human muscle holo-FABP	1.2	2HMB
Rat intestinal apo-FABP	1.4	1IFB
Human apo-CRABP I	1.4	1CBI

[a] r.m.s.d. was calculated with the TOP3D program of the CCP4 package (28).

be the endogenous ligand of these two putative CRBPs, the demonstration that these proteins bind the vitamin physiologically is still lacking. The evidence that retinol is their endogenous ligand is based upon the following observations. Amino acid sequence analyses have revealed a significantly higher identity with the CRBP family members than with the other iLBPs. The binding of retinol to the apoproteins has been reported to produce an absorption spectrum typical of a retinol-CRBP complex in the case of human CRBP III (20) and an increase in retinol fluorescence in the case of murine CRBP III (22). The x-ray molecular model of CRBP III closely resembles the CRBP I and II molecular models (20). Despite the replacement of Gln^{108}, which is hydrogen-bonded to retinol in holo-CRBP I and II (5, 6), by a His residue in human CRBP III, the side chain of this residue is properly positioned within the binding cavity of apo-CRBP III, such that it has the potential to hydrogen bond the vitamin in the holoprotein (20). A binding protein, human CRBP IV, which is related most closely to murine CRBP III, is shown here to belong to a distinct CRBP subfamily and to exhibit rather distinct ligand binding properties.

The recent completion of the draft sequence of the human genome has allowed the analysis of the gene structure organization for the human CRBP types, including human CRBP IV. The gene structure organization for human CRBPs is very similar to that reported for both CRABPs (38) and FABPs (39) and consists of three exons of similar size separated by four introns of variable size. Notably, the size of translated exon sequences and intron position for the human CRBP IV gene are virtually identical to those of the other human CRBP genes. A phylogenetic tree for CRBPs has also been obtained, showing the relationships between a number of CRBPs. While being consistent with the existence of a clear phylogenetic relatedness among a number of binding proteins that may thus be associated with the CRBP family, taken together, these data support the notion that such proteins, including those from remote species, belong to clearly distinct CRBP subfamilies.

A rather low binding affinity of human CRBP IV for all-*trans*-retinol, as compared with the other CRBP types, has been determined in both direct and competitive binding assays. The estimated K_d value for CRBP IV (K_d = ~200 nM) is significantly higher that those determined previously for mammalian CRBP I (K_d as low as 0.1 nM; Refs. 40 and 41), CRBP II (K_d = ~10 nM; Ref. 42), and CRBP III (K_d = ~60 nM; Ref. 20) and is more similar to that reported for the orthologous murine CRBP III (K_d = ~109 nM; Ref. 22). After incubation with CRBP IV, the synthetic retinoid 13-*cis*-retinol gives rise to an UV-visible absorption spectrum close to that of the all-*trans*-retinol-CRBP IV complex, albeit red-shifted by about 5 nm (data not shown). It is worth noting that a similar red shift is also observed for the spectrum of the 13-*cis*-retinol-CRBP I complex compared with that of the all-*trans*-retinol-CRBP I complex. Instead, the spectra obtained with all-*trans*- and 13-*cis*-retinaldehyde and all-*trans*-retinoic acid were close to those of the unbound compounds in the aqueous medium. These results are consistent with the observation that 13-*cis*-retinol binds to murine CRBP III, whereas retinoic acid and retinaldehyde isomers, as well as fatty acids, fail to bind to this binding protein (22).

At variance with the tissue distribution of murine CRBP III mRNA, for which heart, skeletal muscle, adipose tissue, and mammary gland have been found to be the richest organs (21, 22), the highest mRNA level for the orthologous human CRBP IV has been found in adult kidney, and the next richest tissues were adult heart, adult transverse colon, fetal heart, and fetal spleen. It is worth considering, however, that distinct mRNA tissue distributions for another CRBP type (CRBP I) were also observed in humans (20) and the rat (1). Instead, in both humans and the rat, CRBP II mRNA expression is confined essentially to the small intestine (1, 20). The finding that

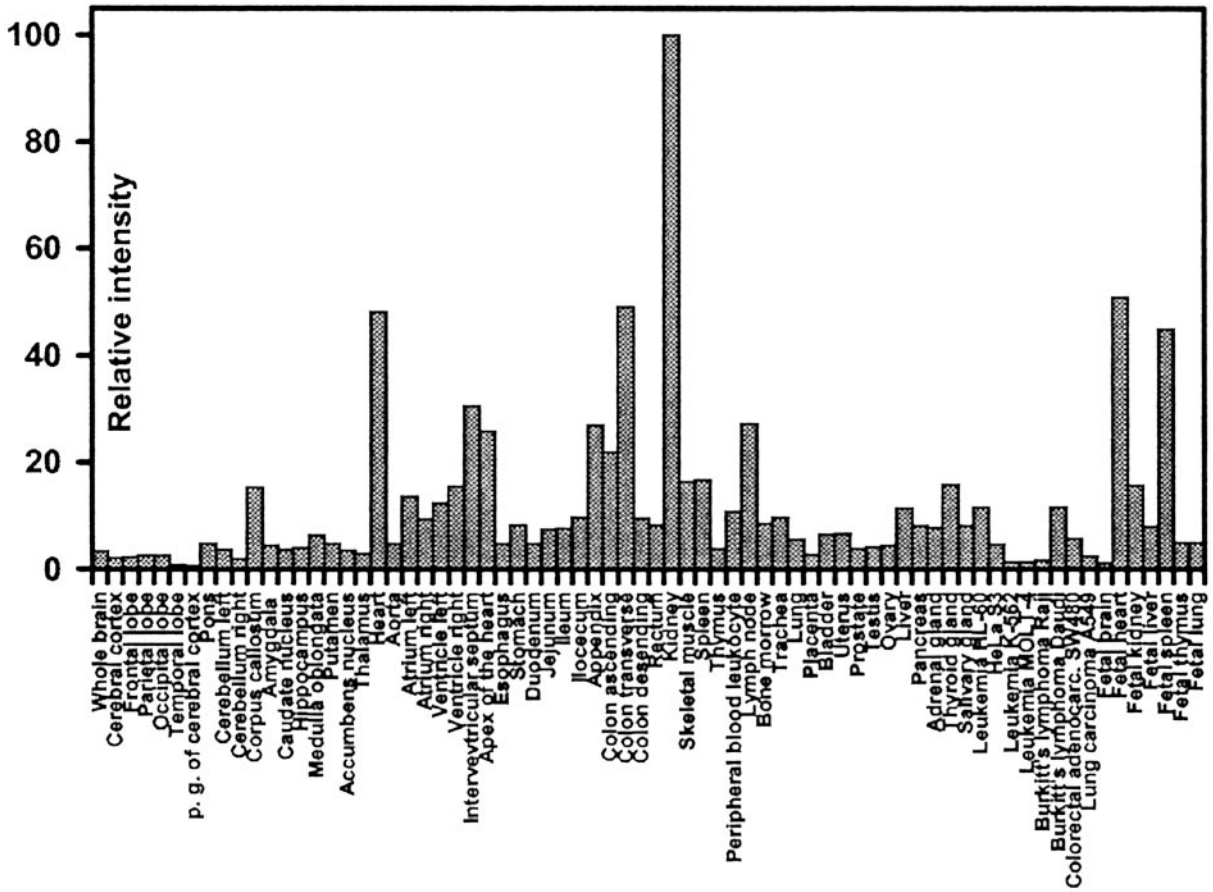

FIG. 7. **Distribution of CRBP IV mRNA in human tissues.** 64 different human tissues and 8 tumor cell lines were analyzed by means of a dot-blot experiment. The results of the experiment are presented as hybridization intensities relative to the maximum hybridization intensity measured.

human kidney contains the highest messenger levels of both CRBP III (20) and CRBP IV points to distinct roles for these two putative CRBPs concomitantly present in this organ.

The apo and holo structures of rat CRBP I and II have been determined previously. Whereas the analysis of the solution structure of rat CRBP I (9) and the x-ray structure of rat CRBP II (6) did not reveal significant structural differences between the apo and holo states of these two proteins, conformational changes affecting several protein regions have been reported for rat CRBP II in solution (7, 8). Recently, significant conformational differences, involving βC-βD and βE-βF turns, have been found for the apo and holo crystal structures of a zebrafish CRBP (34). Consistent with the existence of a remarkable amino acid sequence identity between human CRBP IV and the other CRBP family members, the tertiary structure of human apo-CRBP IV is highly similar to those of previously characterized CRBPs. As in the case of other CRBPs, crystals suitable for x-ray diffraction were obtained from bacterially expressed CRBP IV not supplemented with any ligand during purification and crystallization procedures. However, a continuous electron density was visible inside the central cavity of the β-barrel of apo-CRBP IV, as also observed in the case of human apo-CRBP III (20). This density is likely to be due to the presence in the binding cavity of nonspecific, possibly hydrophobic, ligand/ligands to which CRBP IV became exposed during heterologous expression. Due to the partial occupancy of the retinol-binding site by such compounds in place of the endogenous ligand, the structure of the presumed apo form of CRBP IV we have obtained is likely to be more similar to that of a holoprotein than to that of an apoprotein.

Because of the instability of the retinol-CRBP IV complex during the course of protein crystallization, crystals of holo-CRBP IV could not be obtained, and therefore, the mode of binding of retinol to CRBP IV could not be established on a structural basis. The finding of an absorption spectrum of holo-CRBP IV rather different from those of the other holo-CRBPs suggests a relatively different mode of binding of the vitamin. Consistent with the results of binding experiments with the CRBP I/Q108H and CRBP IV/H108Q mutants, the modification of the absorption spectrum of the retinol-CRBP IV complex is not attributable to the presence of a His residue at position 108. The crystal structure of apo-CRBP IV has revealed a position of the side chain of Tyr^{60} incompatible with the orientation of the retinol β-ionone ring, within the binding cavity, that has been established previously for holo-CRBP I and II (5, 6). An accommodation of the β-ionone ring inside the binding cavity compatible with the presence of the Tyr^{60} side chain might be responsible for the observed modification of the holo-CRBP IV absorption spectrum. However, it is worth mentioning that in the case of a crystalline zebrafish, apo-CRBP side chains of residues of β-turns βC-βD and βE-βF, as well as the side chain of Tyr^{60}, are present within the cavity of the apoprotein and that such side chains are displaced from the binding cavity on ligand binding (34). A similar conformational change, albeit limited to the side chain of Tyr^{60}, might also accompany the binding of retinol to human apo-CRBP IV. A rather distinct mode of binding of retinol to CRBP IV, together with a moderately low binding affinity, might represent a peculiar property of this binding protein.

Acknowledgments—We are grateful to the staff of the ID-29 beam line of European Synchrotron Radiation Facility for technical assist-

ance during x-ray data collection. We thank R. Percudani for skillful assistance with sequence analysis and D. Bellovino for the CRBP I cDNA.

REFERENCES

1. Ong, D. E., Newcomer, M. E., and Chytil, F. (1994) in *The Retinoids: Biology, Chemistry and Medicine* (Sporn, M. B., Roberts, A. B., and Goodman, D. S., eds), pp. 283–318, Raven Press Ltd., New York
2. Li, E., and Norris, A. W. (1996) *Annu. Rev. Nutr.* **16,** 205–234
3. Banaszak, L., Winter, N., Xu, Z., Bernlohr, D. A., Cowan, S., and Jones, T. A. (1994) *Adv. Protein Chem.* **45,** 89–151
4. Newcomer, M. E., Jamison, R. S., and Ong, D. E. (1998) *Subcell. Biochem.* **30,** 53–80
5. Cowan, S. W., Newcomer, M. E., and Jones, T. A. (1993) *J. Mol. Biol.* **230,** 1225–1246
6. Winter, N. S., Bratt, J. M., and Banaszak, L. J. (1993) *J. Mol. Biol.* **230,** 1247–1259
7. Lu, J. Y., Lin, C. L., Tang, C. G., Ponder, J. W., Kao, J. L. F., Cistola, D. P., and Li, E. (1999) *J. Mol. Biol.* **286,** 1179–1195
8. Lu, J. Y., Lin, C. L., Tang, C. G., Ponder, J. W., Kao, J. L. F., Cistola, D. P., and Li, E. (2000) *J. Mol. Biol.* **300,** 619–632
9. Franzoni, L., Lücke, C., Pérez, C., Cavazzini, D., Rademacher, M., Ludwig, C., Spisni, A., Rossi, G. L., and Rüterjans, H. (2002) *J. Biol. Chem.* **277,** 21983–21997
10. Ottonello, S., Petrucco, S., and Maraini, G. (1987) *J. Biol. Chem.* **262,** 3975–3981
11. Troen, G., Nilsson, A., Norum, K. R., and Blomhoff, R. (1994) *Biochem. J.* **300,** 793–798
12. Sundaram, M., Sivaprasadarao, A., DeSousa, M. M., and Findlay, J. B. (1998) *J. Biol. Chem.* **273,** 3336–3342
13. Ong, D. E., McDonald, P. N., and Gubitosi, M. (1988) *J. Biol. Chem.* **263,** 5789–5796
14. Yost, R. W., Harrison, E. H., and Ross, A. C. (1988) *J. Biol. Chem.* **263,** 18693–18701
15. Herr, F. M., and Ong, D. E. *Biochemistry* **31,** 6748–6755, 1992
16. Boerman, M. H., and Napoli, J. L. (1991) *J. Biol. Chem.* **266,** 22273–22278
17. Ottonello, S., Scita, G., Mantovani, G., Cavazzini, D., and Rossi, G. L. (1993) *J. Biol. Chem.* **268,** 27133–27142
18. Boerman, M. H., and Napoli, J. L. (1996) *J. Biol. Chem.* **271,** 5610–5616
19. Ghyselinck, N. B., Bavik, C., Sapin, V., Mark, M., Bonnier, D., Hindelang, C., Dierich, A., Nilsson, C. B., Hakansson, H., Sauvant, P., Azais-Braesco, V., Frasson, M., Picaud, S., and Chambon, P. (1999) *EMBO J.* **18,** 4903–4914
20. Folli, C., Calderone, V., Ottonello, S., Bolchi, A., Zanotti, G., Stoppini, M., and Berni, R. (2001) *Proc. Natl. Acad. Sci. U. S. A.* **98,** 3710–3715
21. Conforti, L., Tarlton, A., Mack, T. G. A., Mi, W., Buckmaster, E. A., Wagner, D., Perry, V. H., and Coleman M. P. (2000) *Proc. Natl. Acad. Sci. U. S. A.* **97,** 11377–11382
22. Vogel, S., Mendelsohn, C. L., Mertz, J. R., Piantedosi, R., Waldburger, C., Gottesman, M. E., and Blaner, W. S. (2001) *J. Biol. Chem.* **276,** 1353–1360
23. Altschul, M., Gish, W., Miller, W., Myers, E. W., and Lipman, D. J. (1990) *J. Mol. Biol.* **215,** 403–410
24. Sanger, F., Nicklen, S., and Coulson, A. R. (1977) *Proc. Natl. Acad. Sci. U. S. A.* **74,** 5463–5467
25. Malpeli, G., Folli, C., Cavazzini, D., Sartori, G., and Berni, R. (1998) in *Methods in Molecular Biology: Retinoids Protocols* (Redfern, C. P. F., ed), Vol. 89, pp. 111–122, Humana Press, Totowa, NJ
26. Gill, S. C., and von-Hippel, P. H. (1989) *Anal. Biochem.* **182,** 319–326
27. Thompson, J. D., Higgins, D. G., and Gibson, T. J. (1994) *Nucleic Acids Res.* **22,** 4673–4680
28. CCP4 Collaborative Project (1994) *Acta Crystallogr.* **D50,** 760–763
29. Navaza, J. (1994) *Acta Crystallogr.* **A50**, 157–163
30. Brünger, A. T., Adams, P. D., Clore, G. M., DeLano, W. L., Gros, P., Grosse-Kunstleve, R. W., Jiang, J.-S., Kuszewski, J., Nilges, M., Pannu, N. S., Read, R. J., Rice, L. M., Simonson, T., and Warren, G. L. (1998) *Acta Crystallogr.* **D54**, 905–921
31. Sheldrick, G. M., and Schneider, T. R. (1997) in *Methods in Enzymology* (Sweet R. M., and Carter, C. W., Jr., eds), Vol. 277, pp. 319–343, Academic Press, Orlando, FL
32. McRee, D. E. (1999) *J. Struct. Biol.* **125,** 156–165
33. Laskowski, R. A., MacArthur, M. W., Moss, D. S., and Thornton, J. M. (1993) *J. Appl. Crystallogr.* **25,** 283–291
34. Calderone, V., Folli, C., Marchesani, A., Berni, R., and Zanotti, G. (2002) *J. Mol. Biol.* **321,** 527–535
35. Werten, P. J. L., Röll, B., van Alten, D. M. F., and de Jong, W. W. (2000) *Proc. Natl. Acad. Sci. U. S. A.* **97,** 3282–3287
36. Ong, D. E., and Chytil, F. (1978) *J. Biol. Chem.* **253,** 828–832
37. Ong, D. E. (1984) *J. Biol. Chem.* **259,** 1476–1482
38. Mansfield, S. G., Cammer, S., Alexander, S. C., Muehleisen, D. P., Gray, R. S., Tropsha, A., and Bollenbacher, W. E. (1998) *Proc. Natl. Acad. Sci.* U. S. A. **95,** 6825–6830
39. Bernlohr, D. A., Simpson, M. A., Hertzel, A. V., and Banaszak, L. J. (1997) *Annu. Rev. Nutr.* **17,** 277–303
40. Li, E., Qian, S. J., Winter, N. S., d'Avignon, A., Levin, M. S., and Gordon, J. I. (1991) *J. Biol. Chem.* **266,** 3622–3629
41. Malpeli, G., Stoppini, M., Zapponi, M. C., Folli, C., and Berni, R. (1995) *Eur. J. Biochem.* **229,** 486–493
42. Levin, M. S., Locke, B., Yang, N. C., Li, E., and Gordon, J. I. (1988) *J. Biol. Chem.* **263,** 17715–17723

Ligand Binding and Structural Analysis of a Human Putative Cellular Retinol-binding Protein

Claudia Folli, Vito Calderone, Ileana Ramazzina, Giuseppe Zanotti and Rodolfo Berni

J. Biol. Chem. 2002, 277:41970-41977.
doi: 10.1074/jbc.M207124200 originally published online August 9, 2002
